OXFORD

Human Molecular Genetics, 2017, Vol. 26, No. 19 3808–3822

doi: 10.1093/hmg/ddx267
Advance Access Publication Date: 17 July 2017
Original Article

ORIGINAL ARTICLE

MicroRNA-455-3p as a potential peripheral biomarker for Alzheimer's disease

Subodh Kumar[1], Murali Vijayan[1] and P. Hemachandra Reddy[1,2,3,4,5,6,*]

[1]Biomarker Unit, Garrison Institute on Aging, [2]Department of Cell Biology & Biochemistry, [3]Department of Pharmacology & Neuroscience, [4]Department of Neurology, [5]Department of Speech, Language and Hearing Sciences and [6]Department of Public Health, Graduate School of Biomedical Sciences, Texas Tech University Health Sciences Center, Lubbock, TX 79430, USA

*To whom correspondence should be addressed at: Mildred and Shirley L. Garrison Chair in Aging, Cell Biology and Biochemistry, Neuroscience & Pharmacology and Neurology Departments, Texas Tech University Health Sciences Center, 3601 4th Street, MS/9424/4A 124, Lubbock, TX 79430, USA. Tel: 806-743-2393; Fax: 806-743-3636; Email: hemachandra.reddy@ttuhsc.edu

Abstract

The purpose of our study was to identify microRNAs (miRNAs) as early detectable peripheral biomarkers in Alzheimer's disease (AD). To achieve our objective, we assessed miRNAs in serum samples from AD patients and Mild cognitive impairment (MCI) subjects relative to healthy controls. We used Affymetrix microarray analysis and validated differentially expressed miRNAs using qRT-PCR. We further validated miRNA data using AD postmortem brains, amyloid precursor protein transgenic mice and AD cell lines. We identified a gradual upregulation of four miRNAs: miR-455-3p, miR-4668-5p, miR-3613-3p and miR-4674. A fifth miRNA, mir-6722, was down-regulated in persons with AD and mild cognitive impairment compared with controls. Validation analysis by qRT-PCR showed significant upregulation of only miR-455-3p ($P = 0.007$) and miR-4668-5p ($P = 0.016$) in AD patients compared with healthy controls. Furthermore, qRT-PCR analysis of the AD postmortem brains with different Braak stages also showed upregulation of miR-455-3p ($P = 0.016$). However, receiver operating characteristic curves (ROC) curve analysis revealed a significant area under curve (AUC) value only for miR-455-3p in the serum (AUROC = 0.79; $P = 0.015$) and brains (AUROC = 0.86; $P = 0.016$) of AD patients. Expression analysis of amyloid precursor protein transgenic mice also revealed high level of mmu-miR-455-3p ($P = 0.004$) in the cerebral cortex (AD-affected) region of brain and low in the non-affected area, i.e. cerebellum. Furthermore, human and mouse neuroblastoma cells treated with the amyloid-$\beta_{(1–42)}$ peptide also showed a similarly higher expression of miR-455-3p. Functional analysis of differentially expressed miRNAs via the miR-path indicated that miR-455-3p was associated in the regulation of several biological pathways. Genes associated with these pathways were found to have a crucial role in AD pathogenesis. An increase in miR-455-3p expression found in AD patients and Aβ pathologies unveiled its biomarker characteristics and a precise role in AD pathogenesis.

Introduction

Alzheimer's disease (AD) is progressive neurological disorder affecting aged humans (1). The loss of memory, thinking skills, reasoning abilities and changes in personality and in behavior are the main characteristics of AD (2). Currently, over 46.8 million people worldwide, including 5.4 million Americans, live with AD-related dementia, and this number is estimated to increase to 131.5 million by 2050 (2). The major pathological hallmarks of AD are the formation of extracellular amyloid plaques and intracellular neurofibrillary tangles in brains of patients with AD. The amyloid plaques accumulate owing to the overproduction of the amyloid β peptide (Aβ). This overproduction is owing to endoproteolysis of the parental amyloid precursor protein (APP), which is cleaved by the enzyme complexes α-,

Received: May 4, 2017. **Revised:** June 30, 2017. **Accepted:** July 4, 2017

β- and γ-secretases (3). Increased production and reduced clearance of Aβ in the brain, may lead to a cascade of events in disease process, including synaptic damage, hyperphosphorylated tau (p-tau), mitochondrial structural and functional changes, inflammatory responses, hormonal imbalance, cell cycle changes and neuronal loss (4–6).

Currently, to diagnose AD, several biochemical tests are used to detect Aβ and p-tau proteins in the cerebrospinal fluid (CSF) of AD patients. This fluid then undergoes biochemical and molecular tests, to determine the levels of biomarkers of AD. In the CSF of patients diagnosed with AD, the concentration of $A\beta_{(1–42)}$ has been found to be 40–50% lower than concentration levels in individuals who do not have AD (6). Such lower levels of $A\beta_{(1–42)}$ in patients have been detected at later stages of AD progression, but they have not been detected in patients in early stages of disease progression. The use of CSF analysis to determine levels of $A\beta_{(1–42)}$ is considered a safe procedure, but often times, the patients complain about post-examination headaches (7). CSF examination requires highly skilled persons puncturing the lumbar to remove spinal fluid. Additional testing to diagnose AD uses highly sophisticated neuroimaging techniques, such as positron emission tomography and structural magnetic resonance imaging and scanning (8).

Given these problems with diagnostic tests for AD, in the last decade researchers have focused on developing non-invasive diagnostic tests capable of detecting nucleic acids, particularly microRNA (miRNAs), known to regulate in patients with AD. These miRNAs are small nucleotide molecules (~22–25 measurement unit) that expressed in humans, plants, fungi, bacteria and some viruses (9). In neurodegenerative diseases such as AD, miRNAs have been found to be deregulated in the blood, plasma, serum, CSF, extracellular fluid and brain tissues of AD patients (10,11).

In humans, miRNAs are believed to be involved in all developmental and pathological processes by regulating gene expression. They achieve this regulation by targeting 3' UTR and binding RNA sequences at 3'UTR in a sequence-specific manner (12). Some miRNAs are tissue-specific and are localized at certain cellular niches, while others are expressed in all tissues and organs of human body. MiRNAs synthesized in the cells and usually modulate mRNA activity of host cells while in several circumstances, miRNAs released from cells are involved in regulating signals for cells-to-cell communication, known as extracellular miRNAs (13). Extracellular miRNAs are secreted from cells via encapsulated exosomes and micro-particles, or they are released with several lipoprotein complexes, such as high-density lipoproteins, low-density lipoproteins and argonaute 2 proteins (13). These extracellular circulatory miRNAs are very stable in blood components. In pathological conditions, such as in persons with AD, concentrations of particular miRNAs are altered (11). However, we still do not have complete understanding of how expressions(s) of miRNAs progress in non-demented elderly individuals to mild cognitive impairment (MCI), and MCI to AD.

Several recent miRNA studies using CSF, serum, plasma and whole blood revealed that circulatory miRNAs as peripheral biomarkers in AD (6,14–22). However, these studies provided information about miRNAs with little or no consensus in all studies. Furthermore, validation of differentially expressed miRNAs using AD postmortem brains is not well done in these studies. Therefore, a more detailed study on circulatory miRNAs in AD patients and MCI subjects with thorough validation is urgently needed, in order to determine early detectable peripheral biomarkers in AD. In the present study, we sought to determine miRNAs as early detectable biomarkers in serum samples from AD patients, MCI subjects relative to healthy controls. We used Affymetrix microarray analysis and validated differentially expressed miRNAs using qRT-PCR. We further validated the data using AD postmortem brains, APP transgenic mice and AD cell lines.

Results

Primary screening of serum samples to detect miRNAs

AD patients ($n = 10$), MCI subjects ($n = 16$) and controls ($n = 14$) (Table 1) were analyzed for their miRNA microarray expression using the Affymetrix GeneChip miRNA Array, v. 4.0. A total of 6631 genes were detected in all of the serum samples. Of these 6631 genes, 2578 were mature miRNAs that were listed in the miRbase database, and 2025 were the stem-loop precursor miRNAs (pre-miRNAs) (Table 2). The remaining genes belonged to different classes of small RNAs, such as snoRNA (1491), CDBox (319), HAcaBox (155), scaRna (31) and 5.8s rRNA (10). Of the remaining genes, 22 were spike-in control RNAs that were added externally during the array experiment. Differential miRNA expression in each miRNA was analyzed, on the fold-change intensity of each miRNA (−2 to +2) and each ANOVA P-value (<0.05).

AD patients and healthy controls

Microarray analysis was performed on the samples from the AD patients ($n = 10$) and the controls ($n = 14$) (Fig. 1). The miRNA bi-weight average (log2) intensity showed significant ($P < 0.05$) de-regulation of 7 miRNAs in AD patients compared with controls (Table 3). The miRNA sequences, hsa-miR-455-3p, hsa-miR-3613-3p, hsa-miR-4668-5p, hsa-miR-5001-5p, hsa-miR-4674 and hsa-miR-4741, were up-regulated, while hsa-miR-122-5p was down-regulated. The top miRNA candidate was hsa-miR-455-3p, which showed a remarkably 11.3-fold higher expression in AD patients compared with controls. Other miRNAs were hsa-miR-3613-3p (3.67-fold), hsa-miR-4668-5p (3.38-fold) and hsa-miR-4674 (5.62-fold) also exhibited the higher levels of fold expression in AD patients. These results identified new miRNA candidates that were not previously identified in AD.

AD patients and MCI subjects

To compare the intermediate states of disease progression, microarray data were analyzed from the AD patients ($n = 10$) and MCI subjects ($n = 16$). Heat map data and hierarchical clustering showed the differential expressions of eight miRNA candidates (Fig. 2). Based on the bi-weight average (log2) intensity and linear fold-change values, the miRNAs hsa-miR-3613-3p and hsa-miR-4668-5p were significantly up-regulated (ANOVA, $P < 0.05$) and hsa-mir-320d-2, hsa-miR-378h, hsa-miR-3921, hsa-miR-6805-5p, hsa-miR-92a-3p, hsa-miR-3613-5p were down-regulated in the serum samples of AD patients compared with MCI subjects (Supplementary Material, Table S1).

MCI subjects and healthy controls

Microarray data were compared between MCI subjects ($n = 16$) and controls ($n = 14$). Hierarchical clustering showed a wide range of miRNA signatures that were deregulated (Fig. 3). Interestingly, 50 miRNAs were identified, and all of them were significantly up-regulated in MCI subjects (Supplementary Material, Table S2). Surprisingly, miR-4674 (5.24-fold) and miR-455-3p (5.18-fold) showed maximum upregulation in MCI

Table 1. Demographic profile of serum samples

Primary screening and validation						
S. No.	Cog Dx	Age	Gender	APOE genotype	MMSE	Race ethnicity
1	AD	82	M	3/3	20	Hispanic
2	AD	88	F	3/4	28	Caucasian
3	AD	87	F	3/3	12	Caucasian
4	AD	74	F	3/3	24	Hispanic
5	AD	82	M	3/3	19	Black
6	AD	72	M	3/4	25	Black
7	AD	63	F	4/4	21	Caucasian
8	AD	75	F	3/3	24	Caucasian
9	AD	74	M	4/4	25	Caucasian
10	AD	56	M	3/3	26	Hispanic
11	MCI-A-M	69	M	3/3	25	Caucasian
12	MCI-A-S	76	F	3/3	26	Hispanic
13	MCI-A-S	70	F	2/2	24	Caucasian
14	MCI-A-S	77	F	3/4	29	Caucasian
15	MCI-A-S	70	M	3/3	18	Hispanic
16	MCI-A-S	62	M	3/3	21	Hispanic
17	MCI-A-S	75	M	3/4	26	Caucasian
18	MCI-A-M	81	M	2/3	27	Caucasian
19	MCI-NA-S	70	F	3/3	26	Caucasian
20	MCI-A-M	86	F	3/3	27	Caucasian
21	MCI-A-M	63	M	3/3	25	Hispanic
22	MCI-A-S	80	F	3/3	25	Caucasian
23	MCI-A-S	75	M	3/3	27	Caucasian
24	MCI-A-S	65	M	3/4	28	Hispanic
25	MCI-A-S	66	F	3/4	ND	Hispanic
26	MCI-A-S	78	F	3/3	25	Caucasian
27	NC	74	F	3/3	21	Hispanic
28	NC	70	M	3/3	25	Hispanic
29	NC	62	F	3/3	30	Caucasian
30	NC	82	F	3/4	27	Caucasian
31	NC	67	F	4/4	25	Hispanic
32	NC	65	M	2/3	28	Hispanic
33	NC	75	F	3/4	30	Caucasian
34	NC	74	M	3/3	29	Caucasian
35	NC	58	M	3/3	21	Hispanic
36	NC	81	M	3/4	24	Caucasian
37	NC	80	F	3/4	30	Caucasian
38	NC	75	F	3/4	30	Caucasian
39	NC	72	F	4/4	27	Hispanic
40	NC	86	M	2/3	29	Caucasian
Validation						
41	AD	86	M	3/4	27	Caucasian
42	MCI-A-M	73	F	3/3	24	Caucasian
43	MCI-A-M	88	M	3/4	25	Caucasian
44	MCI-A-M	73	F	3/3	28	Caucasian
45	MCI-A-S	85	M	3/3	20	Hispanic
46	NC	84	F	2/3	28	Caucasian
47	NC	88	F	3/3	30	Caucasian
48	NC	84	F	3/3	29	Caucasian
49	NC	65	F	3/3	28	Black

subjects, compared with controls. These results suggested that greater number of miRNA deregulation were observed at the initial phases of disease progression.

AD patients, MCI subjects and healthy controls

To detect disease progression through the differential expression of miRNAs, we compared the differentially expressed miRNAs in the serum samples of AD patients and MCI subjects ($n = 10$ and $n = 16$, respectively) and controls ($n = 14$) at the same time point in disease progression. The miRNAs in each group of serum samples were analyzed in terms of: bi-weight average (log2) intensity, a fold change of less than -2 or more than 2, and an ANOVA/false discovery rate (FDR), $P < 0.05$. Results indicated that a total of 68 miRNAs (32 mature and 36 precursors) were deregulated among three groups of serum samples (Fig. 4). Because, present study aimed to identify promising biomarkers for AD progression, we focused on miRNAs, and those expressions are either gradually increased or decreased among three groups. Of the 32 mature miRNAs that were identified, 7 were gradually upregulated: hsa-miR-455-3p, hsa-miR-3613-3p, hsa-miR-4674, hsa-miR-4668-5p, hsa-miR-4317, hsa-miR-3124-3p and hsa-miR-6856-3p, while one, hsa-miR-1972 was downregulated in AD and MCI subjects compared with controls (Supplementary Material, Table S3). Furthermore, the remaining pre-miRNAs (hsa-mir-124-1, hsa-mir-4417, hsa-mir-1908, hsa-mir-3912, hsa-mir-4325 and hsa-4776-2) showed gradual upregulation while four of the pre-miRNAs (hsa-mir-6722, hsa-mir-412, hsa-mir-3153 and hsa-mir-4430) showed gradual downregulation (Supplementary Material, Table S3).

Among the 68 miRNAs that we studied, the most significantly upregulated (ANOVA/FDR, $P < 0.05$) were 4 miRNAs miR-455-3p, miR-3613-3p, miR-4674 and miR-4668-5p and the one downregulated miRNA mir-6722. These miRNAs were selected for secondary screening and validation analysis because their expression varied more in the three groups of serum samples (Table 4). The miR-455-3p log2 intensity showed a 2.53-fold increase in the controls, a 4.9-fold increase in MCI subjects and a 6.03-fold increase in AD patients. Similarly, the expression of miR-4674 also increased from 1.99-fold in controls, to a 4.38-fold increase in MCI subjects, and to a 4.48-fold increase in AD patients.

The miR-4668-5p showed a gradual upregulation of up to 3-fold in AD patients, compared with 1.25-fold increase in controls, and a 1.67-fold increase in MCI subjects. The miR-3613-3p expression also gradually increased when the miRNAs were analyzed and compared in controls, MCI, and AD patients (1.13-, 1.25- and 3.0-fold increases, respectively). The expression of mir-6722 gradually decreased in MCI subjects (6.27-fold) and AD patients (5.72-fold) compared with mir-6722 expression (6.72-fold) in controls. Thus, the circulatory serum miRNAs showed aberrant expression in the healthy controls and diseased states (AD and MCI). Also noteworthy was that the level of expression in these molecules consistently either increased or decreased with disease progression. Hence, such miRNAs could be candidates for diagnostic tools capable of discriminating between

Table 2. Classes of small RNA genes detected by Affymetrix microarray

Total Number of genes identified by Affymetrix microarray analysis: 6631							
Mature miRNA	Stem-loop/pre miRNAs	snoRNA	CDBox	HAcaBox	scaRna	5.8s rRNA	Spike-in control
2578	2025	1491	319	155	31	10	22

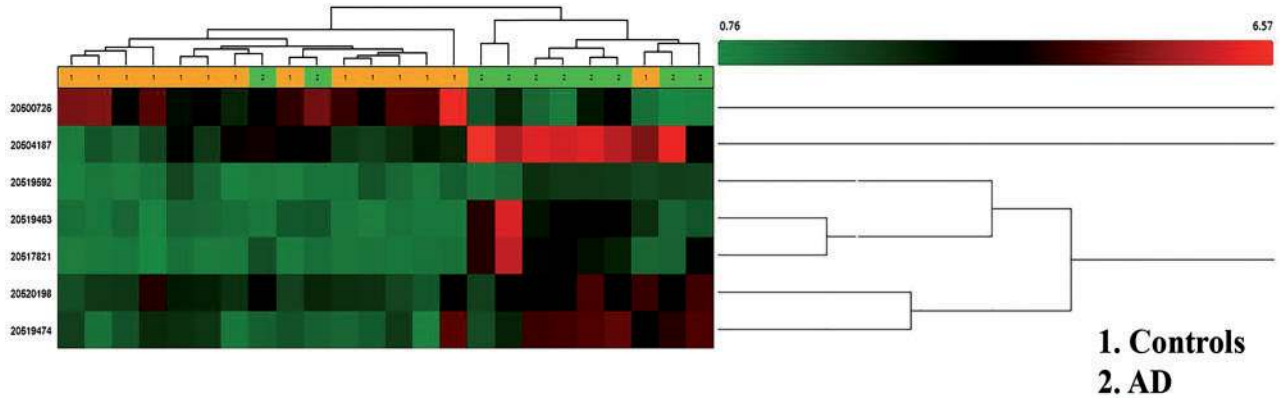

Figure 1. Heat map showing hierarchical clustering of miRNAs in AD patients and healthy controls. Left side showed the transcript cluster ID of differentially expressed seven miRNAs. Red and green color indicate high- and low-expression intensities, respectively.

Table 3. MiRNAs: log2 intensity and fold change in AD patients and controls

Transcript cluster ID	miRNA name	AD Bi-weight average signal (log2)	AD standard deviation	Control bi-weight average signal (log2)	Control standard deviation	Fold change (linear) (AD versus control)	ANOVA P-value	FDR P-value	Chromosome
20504187	hsa-miR-455-3p	6.03	1.05	2.53	1.06	11.3	0.000003	0.007	chr9
20517821	hsa-miR-3613-3p	3	1.32	1.13	0.16	3.67	0.000014	0.012	chr13
20519463	hsa-miR-4668-5p	3	1.5	1.25	0.42	3.38	0.000576	0.079	chr9
20500726	hsa-miR-122-5p	2.31	1.4	4.26	1.24	−3.85	0.004833	0.198	chr18
20520198	hsa-miR-5001-5p	3.73	0.7	2.49	0.77	2.37	0.011848	0.263	chr2
20519474	hsa-miR-4674	4.48	1.37	1.99	1.05	5.62	0.013827	0.275	chr9
20519592	hsa-miR-4741	2.31	0.61	1.26	0.42	2.07	0.013923	0.276	chr18

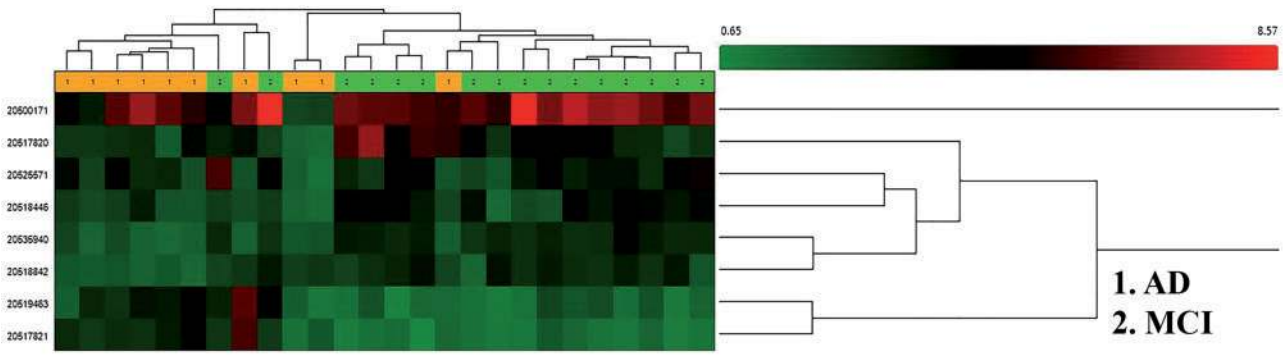

Figure 2. Heat map showing hierarchical clustering of miRNAs in AD patients and MCI subjects. Left side shows the transcript cluster ID of differentially expressed 8 miRNAs. Red and green indicate high- and low-expression intensities, respectively.

healthy persons and persons with AD or MCI. Such miRNAs could also be used to monitor disease progression in AD patients.

Secondary screening and validation of miRNAs in serum samples

Selected miRNAs (miR-455-3p, miR-3613-3p, miR-4674, miR-4668-5p and mir-6722) were further validated for their expression using qRT-PCR assays. The expression of miR-455-3p was quantified in serum of controls ($n = 18$), MCI subjects ($n = 20$) and AD patients ($n = 11$). Interestingly, fold-change (mean ± SD) analysis indicated a gradual upregulation of miR-455-3p in AD patients (0.071 ± 0.078-fold) ($P = 0.007$) compared with the fold-change in MCI subjects (0.034 ± 0.024-fold) and in controls (0.019 ± 0.020-fold) (Fig. 5A). Similarly, the expression of miR-4668-5p was also significantly ($P = 0.016$), upregulated in MCI subjects (2.25 ± 2.78-fold) compared with controls (0.340 ± 0.50-fold) (Fig. 5B). However, miR-4668-5p expression did not show significant elevation in the AD patient's serum (1.50 ± 1.61-fold). In similar way, expressions of miR-4674 and miR-3613-3p also increased in the MCI and AD patients, though it was not significant (Fig. 5C and D).

The expression of precursor miRNA (mir-6722) was also quantified by qRT-PCR, with results showing a gradual down regulation in MCI and AD patients compared with controls, but not significantly (Fig. 5E). So, a microarray-based panel of 5

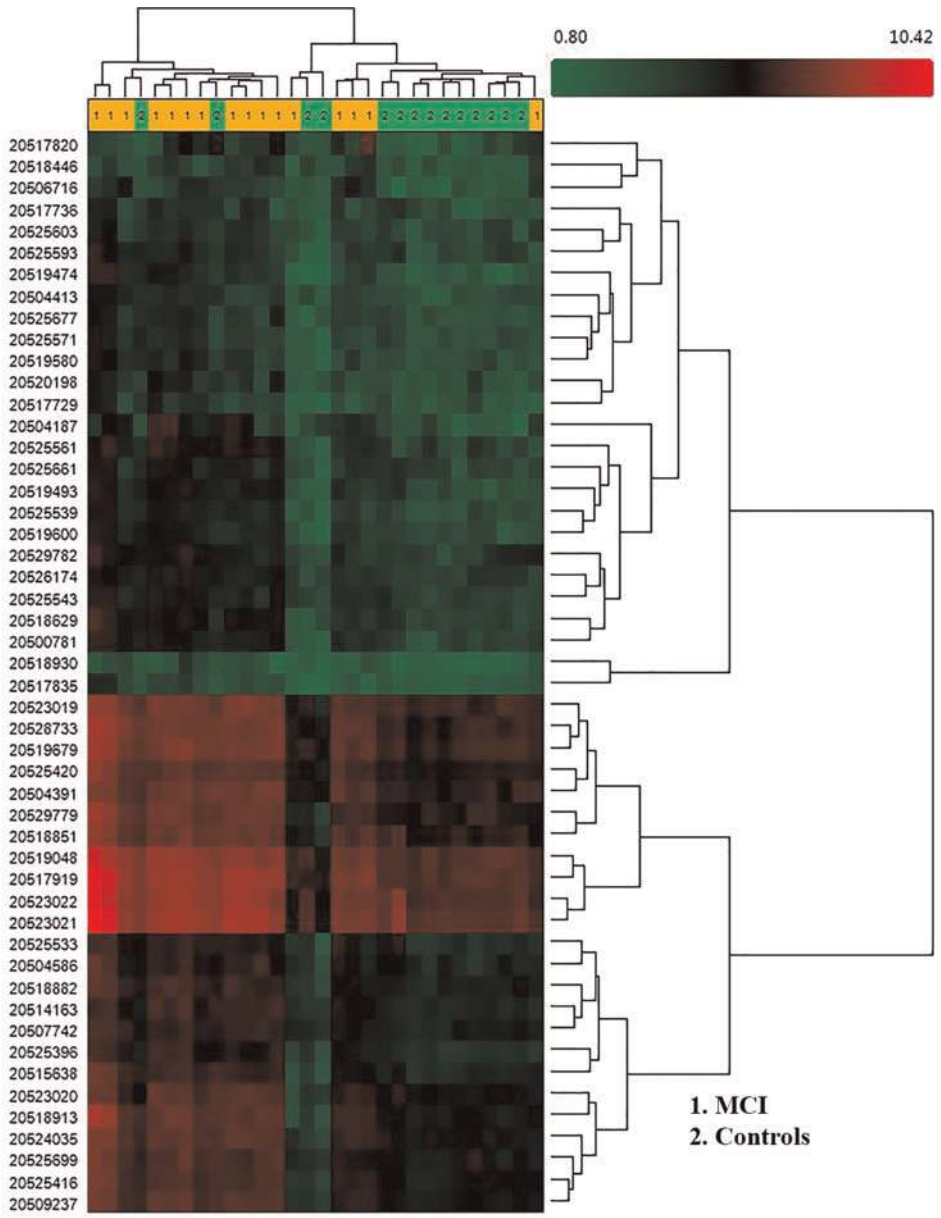

Figure 3. Heat map showing hierarchical clustering of miRNAs in MCI subjects and healthy controls. Left side shows the transcript cluster ID of differentially expressed miRNAs. Red and green indicate high and low expression intensities, respectively.

miRNAs was found to concur with qRT-PCR validation in controls, MCI and AD serum samples. However, our statistical analysis revealed that miR-455-3p and miR-4668-4p were significantly upregulated in persons with AD or MCI from healthy controls.

Validation of serum miRNAs using AD postmortem brains

Total RNA was isolated from postmortem brains (frontal cortex) of AD patients at Braak stages IV ($n = 4$), V ($n = 6$), and VI ($n = 6$), and in controls ($n = 5$) (Table 5). Expression of selected 5-miRNA panel was quantified by qRT-PCR. The average fold change in each miRNA was higher in AD brains at Braak stages IV, V, and VI compared with the control brains. Expression of miR-455-3p was increased in the AD brains at all Braak stages compared with controls. However, a significant upregulation was observed in brains from AD patients at the Braak stage V (26.59-fold, $P = 0.016$) (Fig. 6A). Similarly, miR-3613-3p expression was also higher in the brain tissues at Braak stage V ($P = 0.003$) compared with controls (Fig. 6B).

MiR-4674 expression was also higher in the postmortem brains from AD patients at the Braak stages IV and V, but it was significantly higher at stage VI ($P = 0.003$) (Fig. 6C). MiR-4668-5p expression was also up-regulated in AD brains at Braak stages IV, V, and VI, but not the significant level (Fig. 6D). Mir-6722 expression was down-regulated in AD serum samples. However, the expression of mir-6722 was surprisingly increased in the AD patients at Braak stage VI ($P = 0.018$) (Fig. 6E). The opposite facts were observed in the analysis of mir-6722 expression.

The upregulation of miR-455-3p was significant in postmortem brains from AD patients at Braak stage V. Interestingly,

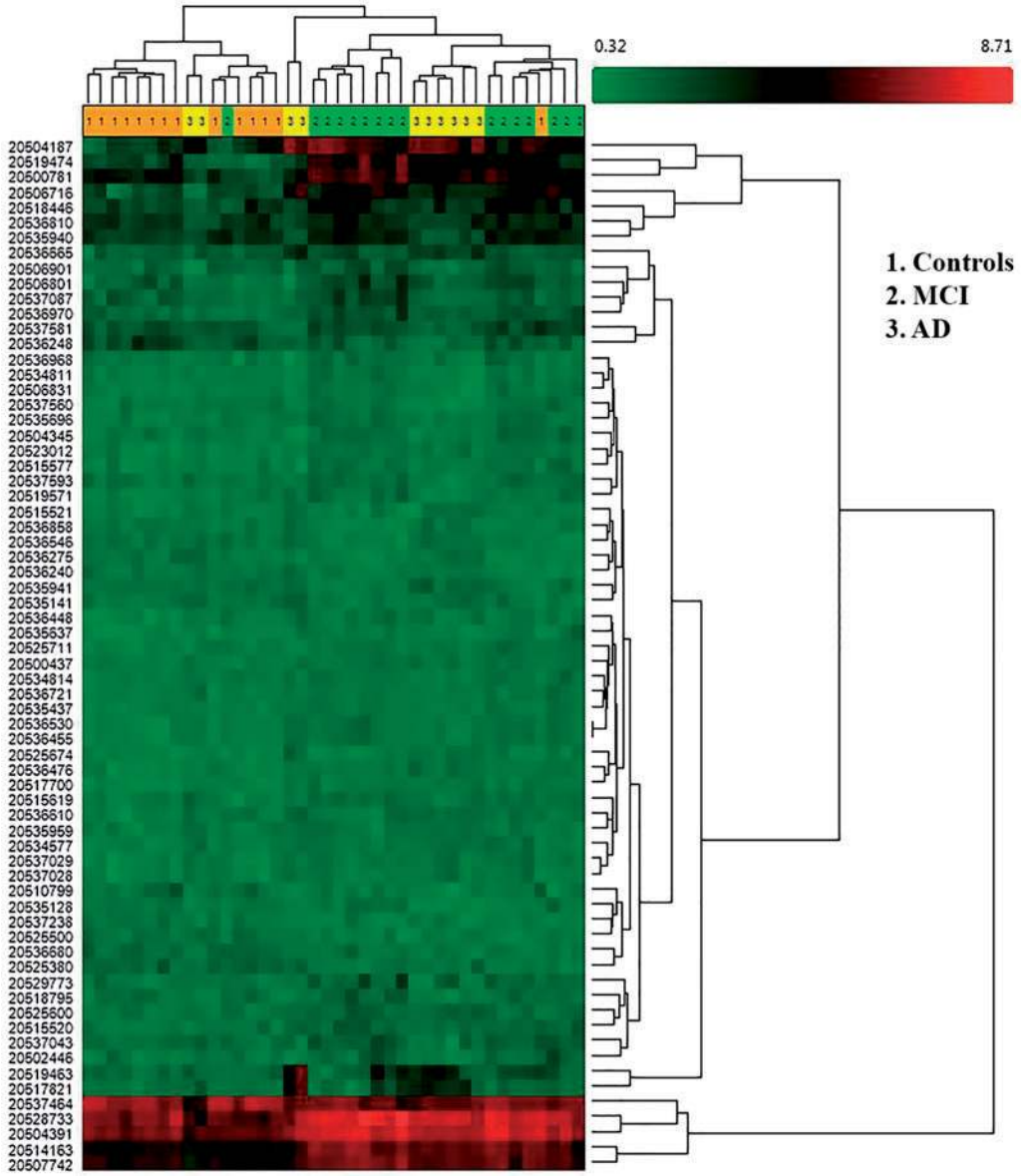

Figure 4. Hierarchical clustering of differentially expressed miRNAs in 40 serum samples (14 controls marked as 1, 14 MCI subjects marked as 2 and 10 AD patients marked as 3 on the top). Left side shows the transcript cluster ID of differentially expressed 63 miRNAs. Red and green color indicate high- and low-expression intensities.

those individuals were all having the ApoE (3/4) genotype (Table 5). The expression of miR-455-3p was the most significantly higher in both the AD serum and AD postmortem brains suggesting that it might be implicated in AD detection and pathogenesis.

Receiver operating characteristics curve analysis

To determine the diagnostic accuracy using miRNAs in AD patients, ROC curves analysis was studied for miR-455-3p expressions in serum and AD brain samples. The curves were plotted, based on the ΔCt value of miR-455-3p expression in serum samples from the AD patients ($n = 11$) and controls ($n = 18$). Upon analysis, miR-455-3p showed significant area under curve (AUC). The AUROC = 0.79 with a 95% confidence interval was 0.59–0.98 ($P = 0.015$) in AD serum samples compared with the healthy controls (Fig. 7A). Further, ROC analysis of miR-455-3p expression in postmortem brains from 16 AD patients and 5 healthy controls indicated the significant AUROC value of 0.86 (95% confidence interval was 0.61 to 1.11, $P = 0.016$) (Fig. 7B). Thus, ROC analysis confirmed miR-455-3p as a valuable molecule capable of discriminating persons with and without AD.

Expression of miR-455-3p in APP transgenic mice

Because miR-455-3p showed promising results in terms of its expression in AD serum samples and AD postmortem brains, miR-455-3p expression was also studied in the cortical tissues from an APP transgenic mouse model of AD (Tg2576 line). This study investigated the mmu-miR-455-3p expression in brain tissues from 6-month-old APP mice ($n = 6$) and C57BL/6 wild-type mice ($n = 6$). Total RNA was extracted from disease-affected

Table 4. miRNAs: log2 intensity and fold change in AD patients, MCI subjects and controls

Transcript cluster ID	Transcript ID	AD bi-weight average signal (log2)	MCI bi-weight average signal (log2)	Controls bi-weight average signal (log2)	AD SD	MCI SD	Controls SD	ANOVA P-value (all conditions)	FDR P-value (all conditions)	Fold change (linear) (AD versus MCI)	Fold change (linear) (AD versus controls)	Fold change (linear) (MCI versus AD)
20504187	hsa-miR-455-3p	6.03	4.9	2.53	1.05	1.29	1.06	0.000002	0.001994	2.18	11.3	−2.18
20537464	hsa-mir-6722	5.72	6.27	6.72	0.45	0.48	0.4	0.000016	0.007169	−1.46	−1.99	1.46
20519474	hsa-miR-4674	4.48	4.38	1.99	1.37	1.26	1.05	0.000208	0.024285	1.07	5.62	−1.07
20517821	hsa-miR-3613-3p	3	1.25	1.13	1.32	0.64	0.16	9.42E-07	0.001562	3.37	3.67	−3.37
20519463	hsa-miR-4668-5p	3	1.67	1.25	1.5	0.91	0.42	0.000711	0.045154	2.52	3.38	−2.52

tissue from the cerebral cortex and non-affected-cerebellum, and mmu-miR-455-3p expression was measured by qRT-PCR. Results showed a 1.8-fold ($P = 0.004$) upregulation of mmu-miR-455-3p in the cerebral cortex tissues of the APP mice, compared with the wild-type mice (Fig. 8A). Interestingly, in cerebellum, mmu-miR-455-3p expression was significantly ($P = 0.018$) reduced in the APP mice (Fig. 8B). Expression of mmu-miR-455-3p was also examined in the serum samples from APP mice. Mmu-miR-455-3p expression was higher in the APP mice serum compared with the wild-type mice, although it was not statistically significant (Fig. 8C). A high level of mmu-miR-455-3p expression in the APP mice confirmed a possible role in Aβ-mediated AD pathogenesis.

MiR-455-3p expression in $a\beta_{(1–42)}$ treated cells

To determine the effects of the Aβ on the expression of miR-455-3p, the SH-SY5Y (human neuroblastoma) and N2a (mouse neuroblastoma) cells were treated with the $A\beta_{(1–42)}$ peptide (20 μM) for 6 h. Total intracellular RNA was extracted and expression of human and mouse miR-455-3p were measured by qRT-PCR. Results showed a 4.1-fold ($P = 0.027$) increase in hsa-miR-455-3p expression in the Aβ-treated SH-SY5Y cells compared with control (untreated) cells (Fig. 9A). Similarly, in N2a cells, mmu-miR-455-3p expression was also upregulated by 3.8-fold ($P = 0.021$) in Aβ-treated cells compared with control cells (Fig. 9B). These results further confirmed the significant response of miR-455-3p in Aβ pathologies.

MiRNA-associated signaling pathways

MiRNA-associated signaling pathways were analyzed using DIANA TOOLS-miRPath algorithm to identify the biological function of these miRNAs and their role in AD pathogenesis. MicroT-CDS files for all five miRNAs were run with a P value <0.05. KEGG pathway analysis unveiled more than 54 biological pathways associated with these miRNAs. This analysis focused on the miR-455-3p and identified possible molecular targets involved in AD pathogenesis. The miRNA analysis identified the relationship of miR-455-3p with 11 biological pathways and associated genes (Fig. 10). The most important signaling pathways were: the ECM-receptor interaction, the adherens junction, the transforming growth factor beta (TGF-β) signaling pathway, the hippo signaling pathway, and the regulation of the actin cytoskeleton. These signaling pathways and some of their genes (THBS1, COL3A1, HSPG2, COL6A1, RUXN1, MYC, Smad2, PLK1 and TNC) were directly associated with AD pathogenesis. The upregulation of miR-455-3p in AD development might be associated with the modulation of the above-mentioned genes. Thus, analysis of the signaling pathways revealed a possible molecular mechanism for how miR-455-3p is involved in AD pathogenesis.

Discussion

Despite the enormous research efforts that have gone into developing ways to diagnose AD at the earliest stages possible, little progress has been made. Perhaps this is at least in partly owing to initial research that focused on personal characteristics of persons who developed AD, such as their life style, body mass index, status of AD-related alleles, their genotypic and phenotypic variations, and environmental factors (11,23,24). This research recently broadened the list of potential

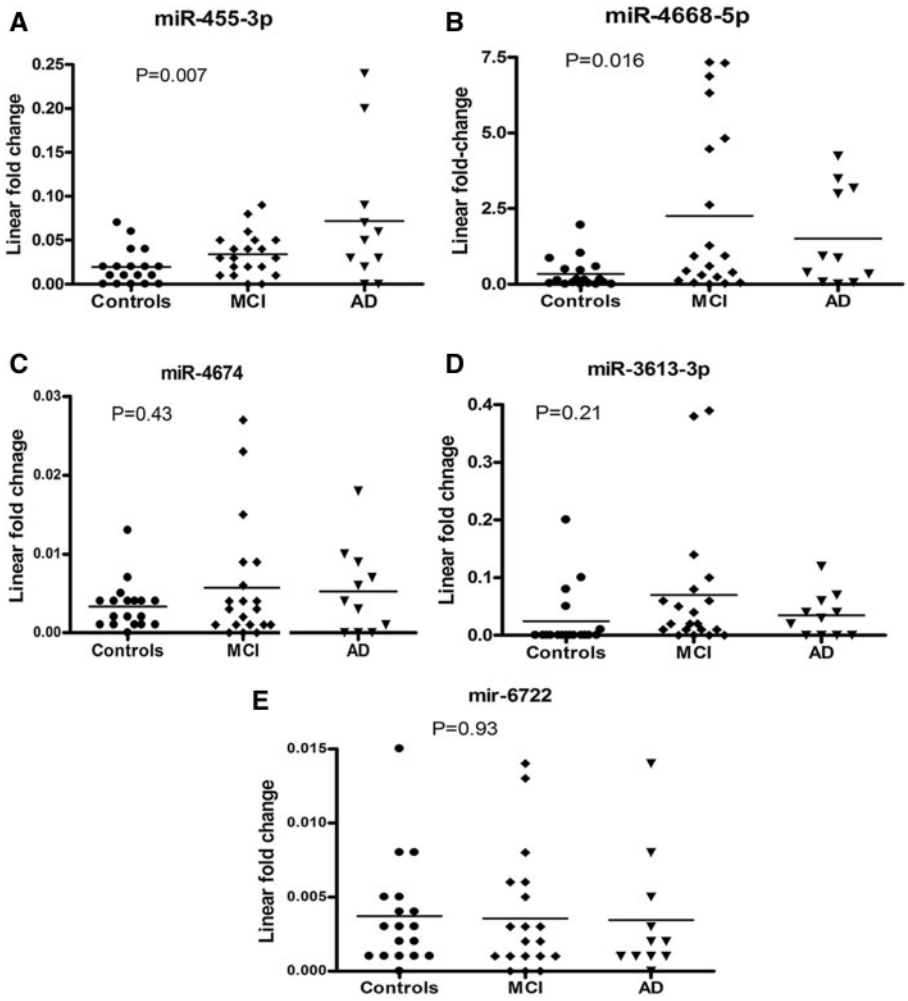

Figure 5. qRT-PCR validation of serum samples. Expression of (**A**) miR-455-3p, (**B**) miR-4668-5p, (**C**) miR-4674, (**D**) miR-3613-3p and (**E**) mir-6722 in healthy controls, MCI subjects and AD patients' serum samples. Fold change was calculated by $2^{-\Delta ct}$ method. Significant difference among groups were calculated by one-way ANOVA with $P < 0.05$ is considered statistically significant.

biomarkers for AD to include blood-based miRNAs, but until the last 5–8 years, little research was actually conducted to narrow the list of miRNAs that might serve as biomarkers for AD, because more than one hundred miRNAs were found to be deregulated in AD patients (6,11,14–21).

The present study is an attempt to narrow the field of miRNAs that might serve as peripheral biomarkers for AD. Using Affymetrix microarray analysis, we identified about 6631 types of small RNAs in the serum of patients with AD and with MCI. Of these, only 2578 were mature, and 2025 were stem-loop precursors of human miRNAs. These numbers of mature miRNAs were almost same as the miRNAs entry on miRbase release 21 (2588 mature) for Homo sapiens (www.mirbase.org/cgi-bin/browse.pl). From these results, we came to know that most of genomic miRNAs were present and/or secreted in peripheral circulation. Based on a recent literature of circulatory miRNAs (11), we had expected that disease-specific miRNAs or miRNAs associated with a particular pathological state, such as AD, were differently expressed and released in peripheral circulation (11). When we compared the 3 different study groups in our research (serum from AD patients, MCI subjects and healthy controls), we found that miRNA expressions of a wide number of miRNAs change, depending on the serum-donor's stage of disease progression. The highest variation of miRNA expressions was found in the patients' serum who were at the initial stage of disease progression, when the diagnosis of these patients went from control to MCI. Hence, disease-specific early physiological changes are crucial for the miRNAs deregulation in cells. Sequencing analysis of serum exosomes unveiled differential expression of 17 miRNAs in the serum from 3 subject groups (17). However, owing to low number of MCI subjects ($n = 11$), none of the exosomal miRNA was verified as biomarker for disease progression (17). In present study, five miRNAs (miR-455-3p, miR-4668-5p, miR-3613-3p, miR-4674 and mir-6722) were selected for validation in order to determine potential biomarker. Results showed a remarkable variation of miR-455-3p in AD serum samples, AD postmortem brains and AD mice, suggesting that it is potential biomarker for AD. These five miRNAs are known to have specific regulating roles in different diseases. MiR-455-3p has a role in colon cancer (25) and also participates in chondrogenic differentiation (26) and cartilage development and degeneration (27). In patients with preeclampsia, miR-455-3p was also found to be linked with hypoxia signaling and the regulation of brown adipogenesis via the HIF1an-AMPK-PGC1a signaling network (28,29). In familial amyotrophic lateral sclerosis, downregulation of miR-455-3p expression has been reported

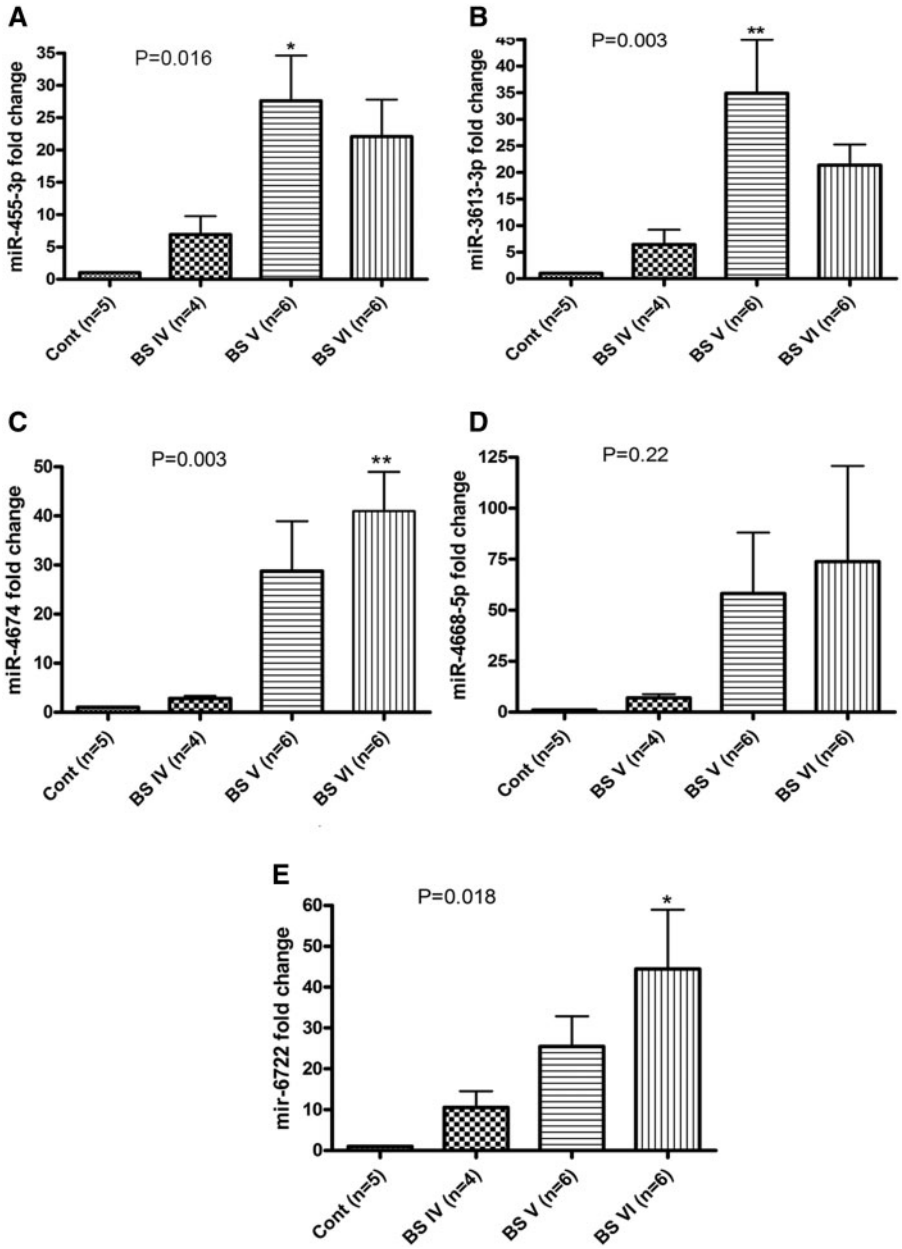

Figure 6. qRT-PCR analysis of AD postmortem brains. Specificity and expression of (A) miR-455-3p, (B) miR-3613-3p, (C) miR-4674, (D) miR-4668-5p and (E) mir-6722 in AD postmortem brain tissues at Braak Stages (BS) IV, V and VI. Fold change was calculated by $2^{-\Delta\Delta ct}$ method. Significant difference among groups were calculated by one-way ANOVA with $P < 0.05$ is considered statistically significant.

in the sera of these patients (30). The roles of miR-3613-3p and miR-4668-5p have been studied in the pathogenesis and progression of IgA nephropathy (31) and in mesial temporal lobe epilepsy (32). In the plasma of AD patients, low levels of miR-3613-3p were detected using RNA sequencing (33). However, current study showed increased levels of miR-3613-3p in the serum samples of AD patients. In hemolysis-free blood plasma from prostatic cancer patients, an increased level of miR-4674 was reported (34). However, role of these miRNAs is not widely reported in AD and other neurodegenerative diseases.

A recent analysis of biofluids (serum, plasma, CSF) from AD patients revealed many miRNA potential biomarkers for AD, such as miR-9, miR-125b, miR-146a, miR-181c, let-7g-5p and miR-191-5p (11). However, their expression levels and molecular characterizations were not investigated using postmortem brains from AD patients and AD cell and mouse models. Consequently, no miRNA has been identified as the most likely biomarker for AD. In this current study, analysis of sera and cortices from AD patients found a significant upregulation of miR-455-3p. We attempted to replicate these observations in AD postmortem brains, APP transgenic mice, and AD cell lines. Interestingly, miR-455-3p expression was more significantly upregulated in the brains and sera from AD patients at Braak stage who had the ApoE (3/4) genotype. These observations unveiled a possible molecular interaction between miR-455-3p and the ApoE4 genotype.

Another significant finding was that APP transgenic mice exhibited Aβ pathologies (35,36) that corresponded to their high

expression of miR-455-3p in the disease-affected brain cortex, but not in other brain areas known not to be affected by disease, such as the cerebellum. These findings indicate a possible molecular link between APP processing and miR-455-3p. This hypothesis was further tested on human and mouse neuroblastoma cells treated with toxic $A\beta_{(1-42)}$ peptides which mimics the AD-type pathophysiology. Higher expression levels of miR-455-3p in the $A\beta_{(1-42)}$-treated cells further support miR-455-3p as a potential biomarker for AD. To the best of our knowledge, our study is the first to identify miR-455-3p as a key molecule expressing biomarker properties for AD. However, additional research into this hypothesis is needed, including an investigation into better understanding the cellular mechanisms underlying how the expression of miR-455-3p responds so quickly to disease process in AD patients.

Table 5. Characteristics of postmortem brain tissues from controls and AD patients

Cases	Gender	Age (years)	Braak Stage	PMI (h)	ApoE
HC1	M	71	–	9	3/4
HC2	M	68	–	6.5	3/4
HC3	F	72	–	11.5	3/3
HC4	F	71	–	7.5	2/2
HC5	M	82	–	6.25	3/3
AD1	M	82	IV	–	3/4
AD2	M	62	IV	5	3/3
AD3	M	78	IV	7.5	3/4
AD4	M	91	IV	8	3/3
AD5	F	77	V	4	3/4
AD6	F	86	V	3.5	3/4
AD7	F	86	V	5	3/4
AD8	F	75	V	4	3/4
AD9	F	80	V	5	3/4
AD10	M	78	V	7	3/4
AD11	M	74	VI	7	3/4
AD12	F	81	VI	6.25	3/3
AD13	F	83	VI	9.25	3/4
AD14	F	86	VI	6	3/4
AD15	M	84	VI	8	3/3
AD16	M	82	VI	5.25	3/4

MiR-455-3p expression is regulated by the TGF-β (37), and its level of expression has been found to be induced by TGF-β1, TGF-β3, and activin A in human SW-1353 chondrosarcoma cells and murine C3H10T1/2 cells (28). The TGF-β signaling pathway reported to play a critical role in Aβ processing in patients with AD because reduced TGF-β signaling has been found to be increased in Aβ deposits in patients with AD (38,39).

Through pathway analysis, the KEGG pathway was found to regulate the TGF-β signaling pathway and eleven associated genes by miR-455-3p (Fig. 10). As a consequence, miR-455-3p might be interconnected with TGF-β signaling and Aβ synthesis, hence it might also play a crucial role in AD pathogenesis. MiR-455-3p might also have a major regulatory role in other cellular pathways through modulation of their genes in AD pathogenesis (Fig. 7). It is possible that miR-455-3p may be involved in AD progression through altered expressions of HSPG2, THBS1, COL3A1, COL6A1, TNC, MYC, Smad2, RAN, PLK1, TP73, ACTN1 and IQGAP1 genes (39–47). However, further research is needed to understand molecular links between miR-455-3p and AD progression.

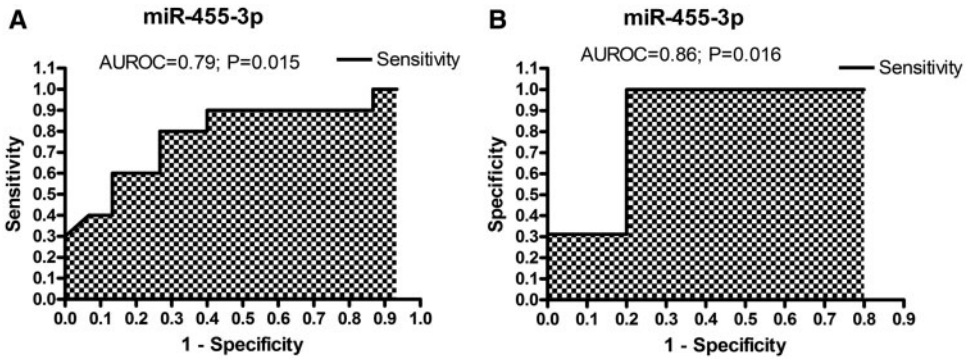

Figure 7. Specificity and sensitivity analysis. ROC curve analysis of miR-455-3p in (**A**) serum samples from AD patients and (**B**) AD postmortem brain tissue samples.

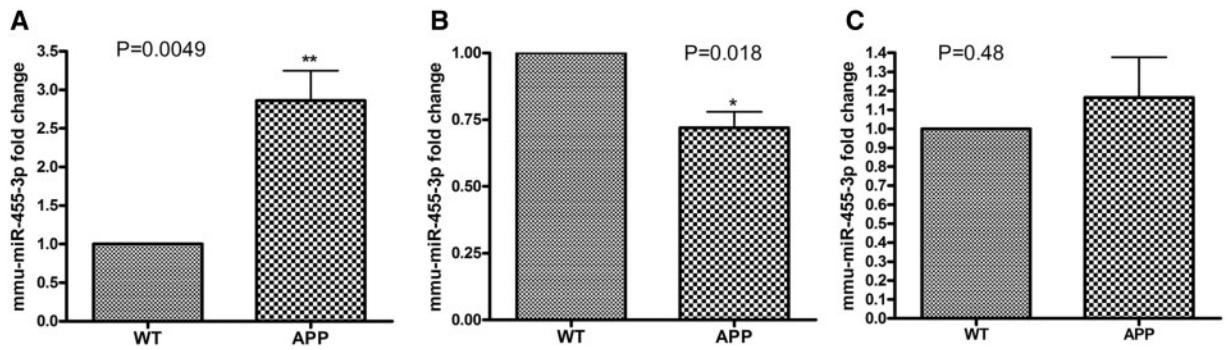

Figure 8. qRT-PCR analysis of miR-455-3p in mice model. mmu-miR-455-3p expression in (**A**) cerebral cortex, (**B**) cerebellum and (**C**) serum of APP-mice compared with wild-type mice. Fold change was calculated by $2^{-\Delta\Delta ct}$ method. Significant difference among groups were calculated by paired *t*-test with two-tailed $P < 0.05$ is considered significant.

In summary, the detection of AD at the preclinical stage is difficult owing to the lack of early detectable peripheral biomarkers. Circulatory miRNAs in sera are potential candidates for early detection of AD because their expressions change during the course of disease progression. Several reports have identified miRNAs as biomarker candidates for AD detection, but as yet, no single miRNA has been clinically verified as an effective biomarker. Our microarray analysis of serum samples revealed a significant upregulation of miR-455-3p expression—an upregulation that correlated in the brain tissues from AD patients, APP transgenic mice and AD cell lines. The findings reported in this paper provide new information about miR-455-3p expression, suggesting a potential role for miR-455-3p as a peripheral biomarker.

Materials and Methods

Study subjects

Sera and DNA samples were collected from patients under the FRONTIERS project based at Garrison Institute on Aging (GIA), Texas Tech University Health Sciences Center (TTUHSC). These samples were obtained from 11 patients diagnosed with AD, 20 patients with MCI and 18 healthy controls. The study protocol was approved by the Institutional Review Board for FRONTIERS, and all subjects provided informed written consent. All the biospecimens were stored at GIA Bio-Bank. Patient information on demographic characteristics, medical history, biochemical profiles and their risk factors for AD was gathered with a standardized questionnaire. Demographic and clinical characteristics of subjects are listed in Table 1. After completing the questionnaire, all subjects underwent a detailed clinical examination to evaluate them for inclusion and exclusion criteria established by NINCDS-ADRDA. The inclusion criteria were: (i) 45 years and above age, (ii) rural community based West Texas individuals and (iii) all study participants have assessed for cognitive functions. The exclusion criteria were: (i) individuals with strong medication and (ii) too many health complications.

MiRNAs extraction

MiRNAs, including other small RNAs, were extracted from the serum samples with the miReasy serum/plasma kit (Qiagen, Germany) as per manufacturer's instructions (16). Briefly, 200 µl of serum samples were mixed with five volumes of a Qiazol lysis

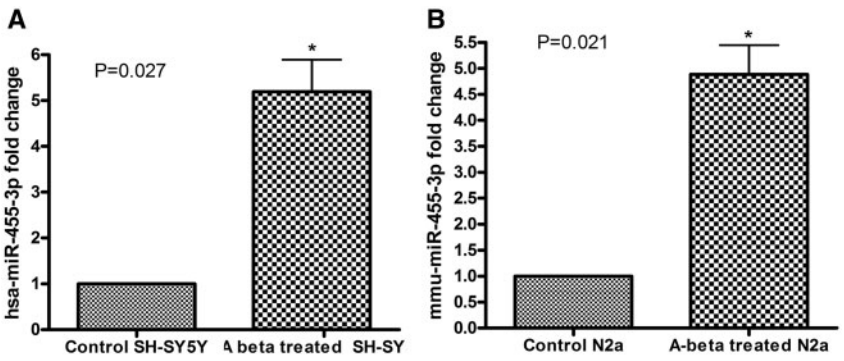

Figure 9. MiR-455-3p expression in cell lines. qRT-PCR analysis of hsa-miR-455-3p expression in (**A**) SHSY-5Y cells, and (**B**) mmu-miR-455-3p expression in N2a cells. Fold change was calculated by $2^{-\Delta\Delta ct}$ method. Significant difference among groups were calculated by paired *t*-test with two-tailed $P < 0.05$ is considered significant.

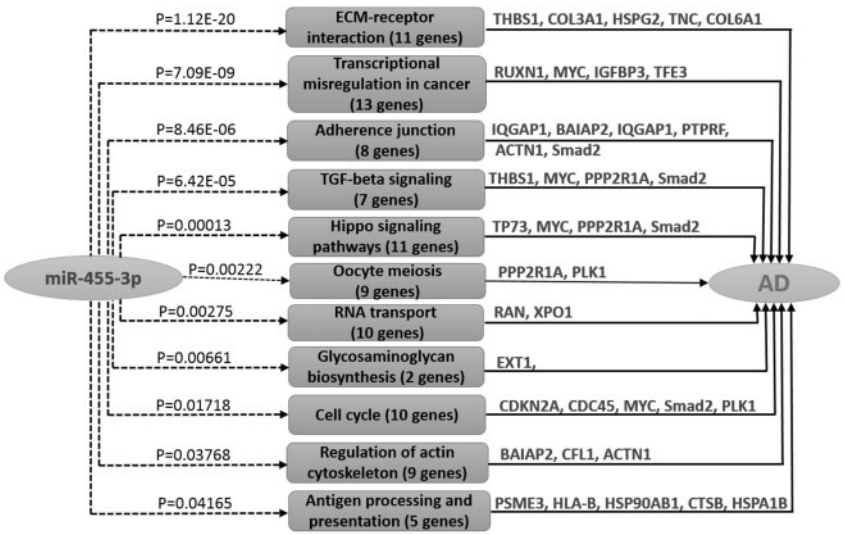

Figure 10. KEGG pathway analysis of miR-455-3p. MiR-455-3p regulated pathways and target genes were identified using the sources microT-CDS and TarBase to classify KEGG pathway and GO category pathway with $P < 0.05$. MiR-455-3p targeted pathway genes identified through literature survey that were implicated in AD pathogenesis.

Table 6. Summary of qRT-PCR oligonucleotide primers used in measuring miRNA expression

miRNA	DNA Sequence (5' to 3')	Base pairs
Hsa-miR-455-3p	Forward primer GCAGTCCATGGGCATATACAC	68
Mmu-miR-455-3p	Forward primer GCAGTCCACGGGCATATACAC	68
Hsa-miR-4674-3p	Forward primer CTGGGCTCGGGACGCGCGGCT	68
Hsa-miR-4668-5p	Forward primer AGGGAAAAAAAAAAGGATTTGTC	70
Hsa-miR-3613-3p	Forward primer ACAAAAAAAAAAGCCCAACCCTTC	71
Hsa-mir-6722	Forward primer GGCCTCAGGCAGGCGCACCCGA Reverse primer GGGTGGGCCAGGCTGTGGGGCG	78
U6 snRNA	Forward primer CGCTTCGGCAGCACATATACTAA Reverse primer TATGGAACGCTTCACGAATTTGC	75
snoRNA-202	Forward primer AGTACTTTTGAACCCTTTTCCA	69

reagent and an equal volume of chloroform, and centrifuged to separate the aqueous phase. MiRNAs accumulated in the aqueous phase were precipitated with 100% ethanol. MiRNAs were washed with a buffer and 80% ethanol, and purified miRNAs were eluted in 15 μl of RNase-free water. RNA quality and quantity were measured by NanoDrop2000c (Thermo Scientific, USA).

Levels of serum miRNAs

Total RNA was extracted from 40 serum sample for microarray analysis, the concentration of miRNAs (10–40 nucleotides) and small RNAs (0–257 nucleotides), and the ratio of miRNAs to small RNAs in each sample were analyzed. The RNA levels were calculated by an Agilent 2100 Bioanalyzer (Agilent Technologies) (Supplementary Material, Fig. S1). The average concentration of miRNAs in AD patients was 89.1 pg/μl, in MCI subjects, 132.7 pg/μl and in controls was 119.3 pg/μl. The average concentration of small RNAs was 186 pg/μl in AD patients, 248.5 pg/μl in MCI subjects and 240.2 pg/μl in controls. Similarly, the ratios of average miRNAs to small RNAs in the samples were 49.1, 54.9 and 49.8% in AD patients, MCI subjects and in controls, respectively (Supplementary Material, Table S4). These results indicated that miRNA output was greater in the MCI subjects.

Primary miRNAs screening by Affymetrix microarray

Detailed miRNAs screening of the serum samples were conducted in the University of Texas Southwestern Medical Center, Genomics and Microarray Core Facility, Dallas. The miRNA expression profiles were generated with Affymetrix GeneChip miRNA array v. 4.0 (Affymetrix). The GeneChip miRNA 2.0 arrays contain a 100% miRBase version 20 coverage: 30 424 mature miRNAs were from all organism; 5214 from human, rat and mouse miRNAs; and 1996 from human snoRNA and scaRNA. It also provided 3770 probe sets that are unique to human, mouse and rat pre-miRNA hairpin sequences. The GeneChip miRNA 4.0 array demonstrated superior performance with 0.95 reproducibility (inter- and intra-lot) and >80% of transcripts were detected at 1.3 amol from 130 ng of total RNA. Data were represented by the GeneChip miRNA 4.0 array in 4 logs that correlated with a dynamic range of >0.97 signal and >0.94-fold change.

Briefly, 8 μl of total RNA was treated for poly (A) tailing reaction at 37°C for 15 min as per the protocol. A 4 μl of 5× Flash Tag Biotin HSR ligation mix was added to poly (A) tailed RNA, and the mixture was incubated at 25°C for 30 min, using the Flash Tag Biotin HSR Labeling kit following the manufacturer's instructions (cat. no. HSR30FTA; Genisphere, LLC, Hatfield, PA, USA). Biotin HSR that labeled with RNA was mixed with an array hybridization cocktail according to the GeneChip Eukaryotic Hybridization control kit manual and was processed using the Affymetrix GeneChip miRNA array. Samples were incubated on the hybridization array chip at 48°C and 60 rpm for 16–18 h. After hybridization, the chips were washed and stained by GeneChip hybridization, washed again and then stained with an Affymetrix kit according to the manufacturer's protocols. The hybridized chips were scanned with an Affymetrix GCS 3000 7G Scanner (48).

Microarray data analysis

Raw data were obtained, using the Affymetrix GeneChip array in the form of an individual CHP file. Each sample was then analyzed, using Transcriptome Analysis Console software v. 3. Tukey's bi-weight average (log2) intensity was analyzed with an ANOVA *P*-value (<0.05) and FDR *P*-value (<0.05) for all conditions, for all genes in the samples from AD, MCI and control group. SAM (significance analysis of microarray) with the R package was used to identify differentially expressed miRNA and gene probe sets in samples from the AD patients and the controls. Probe sets were considered biologically significant if the fold changes were 2 (49).

Validation of serum miRNAs expression using qRT-PCR

Polyadenylation

One microgram of total RNA was polyadenylated with an miRNA First-Strand cDNA synthesis kit (Agilent Technologies Inc., CA, USA), following the manufacturer's instructions. Briefly, a polyA reaction was prepared by mixing RNA with 4.0 μl of 5× poly A polymerase buffer, 1.0 μl of rATP (10 mM), 1 μl of *E. coli* poly A polymerase, producing a final volume of 20 μl with RNase-free water. The tube with these components was incubated at 37°C for 30 min, followed another incubation at 95°C for 5 min to terminate the adenylation reaction (50).

cDNA synthesis

Ten microliters of polyadenylated miRNAs were processed for cDNA synthesis with the miRNA First-Strand cDNA synthesis kit (Agilent Technologies Inc.). The following reaction components were combined in a tube: 2 μl of 10× AffinityScript RT buffer, 0.8 μl of dNTP mix (100 mM), 1 μl of RT adaptor primer (10 μM), 1.0 μl of AffinityScript RT/RNase Block enzyme and polyadenylated RNA. The combination resulted in a reaction volume of 20 μl RNase-free water. This reaction mixture was incubated at 55°C for 5 min, then at 25°C for 15 min, followed by an incubation at 42°C for 30 min and a final incubation at 95°C for 5 min in

a Veriti 96 well thermal cycler (Applied Biosystems, USA). Resulting cDNAs were diluted with 20 µl of RNase-free water and stored at 80°C for further analysis.

qRT-PCR for miRNAs

qRT-PCR reaction was performed by preparing a reaction mixture containing 1 µl of miRNA-specific forward primer (10 µm), 1 µl of a universal reverse primer (3.125 µm) (Agilent Technologies Inc., CA, USA), 10 µl of 2X SYBR® Green PCR master mix (Applied Biosystems, NY, USA) and 1 µl of cDNA. To this mixture RNase-free water was added up to a 20 µl final volume. Primers for hsa-miR-455-3p, miR-4674, miR-3613-3p, miR-4668-5p and mir-6722 were synthesized commercially (Integrated DNA Technologies Inc., IA, USA) (Table 6).

To normalize the miRNA expression, U6 snRNA (small nuclear RNA) expression was also quantified in the serum samples, which was used as an internal control. The reaction mixture of each sample was prepared in triplicates. The reaction was set in the 7900HT Fast Real Time PCR System (Applied Biosystems, USA) using following reaction conditions: initial denaturation at 95°C for 5 min, denaturation at 95°C for 10 s, annealing at 60°C for 15 s and extension at 72°C for 25 s. The relative levels of miRNAs in the AD patients versus the controls and versus the MCI subjects were determined in terms of their fold change, using the formula ($2^{-\Delta\Delta Ct}$), where ΔCt was calculated by subtracting Ct of U6snRNA from the Ct of particular miRNAs, and ΔΔCt value was obtained by subtracting ΔCt of particular miRNAs in the controls from the ΔCt of miRNAs in the AD and MCI. qRT-PCR was performed in triplicate, and the data were expressed as the mean ± SD (50,51).

Postmortem brains from AD patients

Postmortem brain tissues were obtained from the GIA Brain Bank. The frontal cortices of the postmortem brains were dissected from the AD patients ($n = 16$) and controls ($n = 5$). Demographic details of study participants were given in Table 5. The study protocol was approved by the Institute Ethical Committee at TTUHSC, and brain tissue was obtained after written informed consent from the deceased's relatives.

MiRNAs extraction and qRT-PCR

MiRNAs extraction and cDNA synthesis were followed as described above, while total RNA was isolated from the 80 mg of frontal cortices using the TriZol RT reagent (Ambion, USA) as per the manufacturer's instructions. Briefly, tissue samples were homogenized in 1 ml of TriZol reagent with Bio-Gen PRO200 Homogenizer (PRO Scientific Inc., CT, USA) in a 2-ml RNase-free tube. Chloroform (0.2 ml) was added to the tissue homogenate, vigorously shaken for 15 s and stored for 5 min at room temperature. The mixture was then centrifuged at 12 000*g* for 15 min at 4°C. The supernatant was transferred to a new tube and precipitated with 0.5 ml of isopropanol for 15 min at room temperature. Samples were centrifuged at 12 000*g* for 10 min at 4°C. The resulting RNA pellet was washed with 1 ml of 75% ethanol and centrifuged at 7500*g* for 5 min at 4°C. The RNA pellet was dried and dissolved in 20 µl of DEPC-treated water. The quality and quantity of the RNA were analyzed by NanoDrop analysis. The value of absorbance of each brain RNA sample (A_{260}/A_{280}) was 1.8–2.0. cDNA was synthesized from 1 µg of RNA using miRNA First-Strand cDNA synthesis kit (Agilent Technologies Inc.). qRT-PCR were analyzed for miR-455-3p, miR-4674, miR-3613-3p, miR-4668-5p and mir-6722 as described previously.

Animal models

Amyloid-β transgenic (APP) mice were generated with the mutant human APP gene 695-amino-acid isoform and a double mutation ($Lys^{670}Asn$ and $Met^{671}Leu$) (35). The APP mouse model exhibits age-dependent Aβ plaques as well as a distribution of Aβ plaques in the cerebral cortex and the hippocampus, but not in the striatum, the deep gray nuclei and the brain stem. Disease in this mouse model parallels AD in that elevated amounts of soluble Aβ correlate with increased free-radical production, and the Aβ plaques evoke a microglial reaction in their immediate vicinity. Cerebral cortex tissues were collected from 6-month-old APP transgenic mice ($n = 6$) and age-matched, non-transgenic wild-type mice ($n = 6$). To determine transgene-positive mice to model the human APP, genotyping was performed in accordance with the TTUHSC Policy on Genotype Tissue Collection, using the DNA prepared from tail biopsy and PCR amplification (35). All mice were observed daily by a veterinary caretaker and also examined twice weekly by laboratory staff. If any mice showed premature signs of neurological deterioration, they were euthanized before experimentation according to euthanasia procedure approved by the TTUHSC-IACUC and were not used in the study.

Amyloid-$\beta_{(1-42)}$ treatment to cell lines

Human neuroblastoma (SH-SY5Y) and mouse neuroblastoma (N2a) cell lines were purchased from American Tissue Type Collection (ATCC) (Virginia, USA). Cells were grown in a medium (1:1) Dulbecco's modified eagle's medium and minimum essential medium, 5% fetal bovine serum, 1× penicillin and streptomycin) at 37°C in a humidified incubator with a 5% CO_2 environment. After the cells were seeded, they were allowed to grow for 24–48 h or until 80% confluence in 6-well plates. They were then used for experimentation. Two different groups of cells were used: (i) untreated SH-SY5Y/N2a cells and (ii) $A\beta_{(1-42)}$ peptide treated SH-SY5Y/N2a cells. They were incubated with the $A\beta_{(1-42)}$ peptide (20 mM final concentration) in triplicate for 6 h. Both groups of cells were harvested after treatment and processed for total RNA extraction and miR-455-3p quantification.

MiRNAs pathway analysis

MiRNAs that were associated with signaling pathways were analyzed with the miRPath v3.0 web server algorithm (52). Briefly, species was defined as 'human, mouse' and miR-455-3p, miR-4674, miR-3613-3p, miR-4668-5p and mir-6722 were entered. MiRNAs that target genes and biological pathways were analyzed, using microT-CDS and TarBase to classify the GO category, the $P < 0.05$ of the KEGG pathway enrichment, and the microT-CDS threshold (0.8). The miRNA-targeted genes in different KEGG molecular pathways were ranked according to their *P*-value. The FDR $P < 0.05$ was considered statistically significant.

Statistical analysis

The qRT-PCR validation analysis was based on the $2^{-\Delta\Delta CT}$ value of genes in each sample from AD, MCI subjects and controls. Statistical analysis was performed with Prism software, v, 6

(La Zolla, CA). *P*-value was calculated, based on the paired and unpaired *t*-tests for analyzing two groups and using one-way comparative analysis of variance (ANOVA) when comparing between more than two groups. $P < 0.05$ was considered statistically significant.

Supplementary Material

Supplementary Material is available at *HMG* online.

Acknowledgements

We sincerely thank Ms Linda Yin, Ms Annette Boles, Ms Kathy Hudson and all field coordinators for their support in collecting cognitive data and blood samples for this study. We also thank all the participants of Project FRONTIER for providing blood specimens.

Conflict of Interest statement. A patenting application is in progress with the content of our study.

Funding

The research presented in this article was supported by the National Institute of Health grants AG042178 and AG47812, and the Garrison Family Foundation.

References

1. Lukiw, J. (2013) Circular RNA (circRNA) in Alzheimer's Disease (AD). *Front. Genet.*, **4**, 307.
2. Reddy, P.H., Tonk, S., Kumar, S., Vijayan, M., Kandimalla, R., Kuruva, C.S. and Reddy, A.P. (2016) A critical evaluation of neuroprotective and neurodegenerative MicroRNAs in Alzheimer's disease. *Biochem. Biophys. Res. Commun.*, **483**, 1156–1165.
3. LaFerla, F.M., Green, K.N. and Oddo, S. (2007) Intracellular amyloid-β in Alzheimer's disease. *Nat. Rev. Neuro*, **8**, 449–509.
4. Mattson, M.P. (2004) Pathways towards and away from Alzheimer's disease. *Nature*, **430**, 631–639.
5. Reddy, P.H., Manczak, M., Mao, P., Calkins, M.J., Reddy, A.P. and Shirendeb, U. (2010) Amyloid-beta and mitochondria in aging and Alzheimer's disease: implications for synaptic damage and cognitive decline. *J. Alzheimers Dis*, **20**, S499–S512.
6. Kumar, P., Dezso, Z., MacKenzie, C., Oestreicher, J., Agoulnik, S., Byrne, M., Bernier, F., Yanagimachi, M., Aoshima, K. and Oda, Y. (2013) Circulating miRNA biomarkers for Alzheimer's disease. *Plos One*, **8**, e69807.
7. Zafari, S., Backes, C., Meese, E. and Keller, A. (2015) Circulating biomarkers panels in Alzheimer's disease. *Gerontology*, **61**, 497–503.
8. Zhao, Y., Bhattacharjee, S., Dua, P., Alexandrov, P.N. and Lukiw, W.J. (2015) microRNA-based biomarkers and the diagnosis of Alzheimer's disease. *Front. Neurol.*, **6**, 162.
9. Bartel, D.P. (2007) MicroRNAs: genomics, biogenesis, mechanism and function. *Cell*, **116**, 281–297.
10. Adlakha, Y.K. and Saini, N. (2014) Brain microRNAs and insights into biological functions and therapeutic potential of brain enriched miRNA-128. *Mol. Cancer*, **13**, 33.
11. Kumar, S. and Reddy, P.H. (2016) Are circulating microRNAs peripheral biomarkers for Alzheimer's disease? *Biochim. Biophys. Acta*, **1862**, 1617–1627.
12. Ha, M. and Kim, V.N. (2015) Regulation of microRNA biogenesis. *Nat. Rev. Mol. Cell. Biol.*, **15**, 509–524.
13. Boon, R.A. and Vickers, K.C. (2007) Intercellular transport of microRNAs. *Arterioscler. Thromb. Vasc. Biol.*, **33**, 186–192.
14. Schipper, H.M., Maes, O.C., Chertkow, H.M. and Wang, E. (2007) microRNA expression in Alzheimer blood mononuclear cells. *Gene Regul. Syst. Biol.*, **20**, 263–274.
15. Alexandrov, P.N., Dua, P., Hill, J.M., Bhattacharjee, S., Zhao, Y. and Lukiw, W.J. (2012) microRNA (miRNA) speciation in Alzheimer's disease (AD) cerebrospinal fluid (CSF) and extracellular fluid (ECF). *Int. J. Biochem. Mol. Biol.*, **3**, 365–373.
16. Geekiyanage, H., Jicha, G.A., Nelson, P.T. and Chan, C. (2012) Blood serum miRNA: non-invasive biomarkers for Alzheimer's disease. *Exp. Neurol.*, **235**, 491–496.
17. Cheng, L., Doecke, J.D., Sharples, R.A., Villemagne, V.L., Fowler, C.J., Rembach, A., Martins, R.N., Rowe, C.C., Macaulay, S.L., Masters, C.L. *et al.* (2015) Prognostic serum miRNA biomarker associated with Alzheimer's disease shows concordance with neuropsychological and neuroimaging assessment. *Mol. Psychiatry*, **20**, 1188–1196.
18. Galimberti, D., Villa, C., Fenoglio, C., Serpente, M., Ghezzi, L., Cioffi, S.M.G., Arighi, A., Fumagalli, G. and Scarpini, E. (2014) Circulating miRNAs as potential biomarkers in Alzheimer's disease. *J. Alz. Dis.*, **42**, 1261–1267.
19. Tan, L., Yu, J.T., Tan, M.S., Liu, Q.Y., Wang, H.F. and Zhang, W. (2014) Circulating miR-125 as a biomarker of Alzheimer's disease. *J. Neurol. Sci.*, **336**, 52–56.
20. Satoh, J., Kino, Y. and Niida, S. (2015) MicroRNA-Seq data analysis pipeline to identify blood biomarkers for Alzheimer's disease from public data. *Biomarker Insights*, **10**, 21–31.
21. Dong, H., Li, J., Huang, L., Chen, X., Li, D., Wang, T., Hu, C., Xu, J., Zhang, C., Zen, K. *et al.* (2015) Serum microRNA profiles serve as novel biomarkers for the diagnosis of Alzheimer's disease. *Dis. Markers*, **2015**, 625659.
22. Williams, J., Smith, F., Kumar, S., Vijayan, M. and Reddy, P.H. (2016) Are microRNAs true sensors of ageing and cellular senescence? *Ageing. Res. Rev.*, **35**, 350–363.
23. Wu, H.J.Y., Ong, K.L., Seeher, K., Armstrong, N.J., Thalamuthu, A., Brodaty, H., Sachdev, P. and Mather, K. (2016) Circulating microRNAs as biomarkers of Alzheimer's disease: a systemic review. *J. Alz. Dis.*, **49**, 755–766.
24. Liu, C.C., Liu, C.C., Kanekiyo, T., Xu, H. and Bu, G. (2013) Apolipoprotein E and Alzheimer disease: risk, mechanisms and therapy. *Nat. Rev. Neurol.*, **9**, 106–118.
25. Zheng, J., Lin, Z., Zhang, L. and Chen, H. (2016) MicroRNA-455-3p inhibits tumor cell proliferation and induces apoptosis in HCT116 human colon cancer cells. *Med. Sci. Monit.*, **22**, 4431–4437.
26. Zhang, Z., Hou, C., Meng, F., Zhao, X., Zhang, Z., Huang, G., Chen, W., Fu, M. and Liao, W. (2015) MiR-455-3p regulates early chondrogenic differentiation via inhibiting Runx2. *FEBS Lett.*, **589**, 3671–3678.
27. Chen, W., Chen, L., Zhang, Z., Meng, F., Huang, G., Sheng, P., Zhang, Z. and Liao, W. (2016) MicroRNA-455-3p modulates cartilage development and degeneration through modification of histone H3 acetylation. *Biochim. Biophys. Acta*, **1863**, 2881–2891.
28. Lalevée, S., Lapaire, O. and Bühler, M. (2014) miR455 is linked to hypoxia signaling and is deregulated in preeclampsia. *Cell Death Dis.*, **5**, e1408.
29. Zhang, H., Guan, M., Townsend, K.L., Huang, T.L., An, D., Yan, X., Xue, R., Schulz, T.J., Winnay, J. and Mori, M. (2015) MicroRNA-455 regulates brown adipogenesis via a novel

HIF1an-AMPK-PGC1α signaling network. *EMBO Rep.*, **16**, 1378–1393.
30. Freischmidt, A., Müller, K., Zondler, L., Weydt, P., Volk, A.E., Božič, A.L., Walter, M., Bonin, M., Mayer, B. and von Arnim, C.A. (2014) Serum microRNAs in patients with genetic amyotrophic lateral sclerosis and pre-manifest mutation carriers. *Brain*, **137**, 2938–2950.
31. Wang, N., Bu, R., Duan, Z., Zhang, X., Chen, P., Li, Z., Wu, J., Cai, G. and Chen, X. (2015) Profiling and initial validation of urinary microRNAs as biomarkers in IgA nephropathy. *PeerJ*, **3**, e990.
32. Yan, S., Zhang, H., Xie, W., Meng, F., Zhang, K., Jiang, Y., Zhang, X. and Zhang, J. (2017) Altered microRNA profiles in plasma exosomes from mesial temporal lobe epilepsy with hippocampal sclerosis. *Oncotarget*, **8**, 4136–4146.
33. Lugli, G., Cohen, A.M., Bennett, D.A., Shah, R.C., Fields, C.J., Hernandez, A.G. and Smalheiser, N.R. (2015) Plasma exosomal miRNAs in persons with and without Alzheimer disease: altered expression and prospects for biomarkers. *PLoS One*, **10**, e0139233.
34. Knyazev, E.N., Samatov, T.R., Fomicheva, K.A., Nyushko, K.M., Alekseev, B.Y. and Shkurnikov, M.Y. (2016) MicroRNA hsa-miR-4674 in hemolysis-free blood plasma is associated with distant metastases of prostatic cancer. *Bull. Exp. Biol. Med.*, **161**, 112–115.
35. Hsiao, K., Chapman, P., Nilsen, S., Eckman, C., Harigaya, Y., Younkin, S., Yang, F. and Cole, G. (1996) Correlative memory deficits, Abeta elevation, and amyloid plaques in transgenic mice. *Science*, **274**, 99–102.
36. Manczak, M., Kandimalla, R., Fry, D., Sesaki, H. and Reddy, P.H. (2016) Protective effects of reduced dynamin-related protein 1 against amyloid beta-induced mitochondrial dysfunction and synaptic damage in Alzheimer's disease. *Hum. Mol. Genet.*, **25**, 4881–4897.
37. Swingler, T.E., Wheeler, G., Carmont, V., Elliott, H.R., Barter, M.J., Abu-Elmagd, M., Donell, S.T., Boot-Handford, R.P., Hajihosseini, M.K. and Münsterberg, A. (2012) The expression and function of microRNAs in chondrogenesis and osteoarthritis. *Arthritis. Rheum.*, **64**, 1909–1919.
38. Das, P. and Golde, T. (2006) Dysfunction of TGF-beta signaling in Alzheimer's disease. *J. Clin. Invest.*, **116**, 2855–2857.
39. von Bernhardi, R., Cornejo, F., Parada, G.E. and Eugenín, J. (2015) Role of TGFβ signaling in the pathogenesis of Alzheimer's disease. *Front. Cell. Neurosci.*, **9**, 426.
40. Ferrer, I. and Blanco, R. (2000) N-myc and c-myc expression in Alzheimer disease, Huntington disease and Parkinson disease. *Brain. Res. Mol. Brain. Res.*, **77**, 270–276.
41. Rosenmann, H., Meiner, Z., Kahana, E., Aladjem, Z., Friedman, G., Ben-Yehuda, A., Grenader, T., Wertman, E. and Abramsky, O. (2004) An association study of a polymorphism in the heparin sulfate proteoglycan gene (perlecan, HSPG2) and Alzheimer's disease. *Am. J. Med. Genet. B Neuropsychiatr. Genet.*, **128B**, 123–125.
42. Lee, H.G., Ueda, M., Zhu, X., Perry, G. and Smith, M.A. (2006) Ectopic expression of phospho-Smad2 in Alzheimer's disease: uncoupling of the transforming growth factor-beta pathway? *J. Neurosci. Res.*, **84**, 1856–1861.
43. Lee, H.G., Casadesus, G., Nunomura, A., Zhu, X., Castellani, R.J., Richardson, S.L., Perry, G., Felsher, D.W., Petersen, R.B. and Smith, M.A. (2009) The neuronal expression of MYC causes a neurodegenerative phenotype in a novel transgenic mouse. *Am. J. Pathol.*, **174**, 891–897.
44. Cheng, J.S., Dubal, D.B., Kim, D.H., Legleiter, J., Cheng, I.H., Yu, G.Q., Tesseur, I., Wyss-Coray, T., Bonaldo, P. and Mucke, L. (2009) Collagen VI protects neurons against Abeta toxicity. *Nat. Neurosci.*, **12**, 119–121.
45. Donovan, L.E., Dammer, E.B., Duong, D.M., Hanfelt, J.J., Levey, A.I., Seyfried, N.T. and Lah, J.J. (2013) Exploring the potential of the platelet membrane proteome as a source of peripheral biomarkers for Alzheimer's disease. *Alzheimers. Res. Ther.*, **5**, 32.
46. Xie, K., Liu, Y., Hao, W., Walter, S., Penke, B., Hartmann, T., Schachner, M. and Fassbender, K. (2013) Tenascin-C deficiency ameliorates Alzheimer's disease-related pathology in mice. *Neurobiol. Aging*, **34**, 2389–2398.
47. Mastroeni, D., Chouliaras, L., Grover, A., Liang, W.S., Hauns, K., Rogers, J. and Coleman, P.D. (2013) Reduced RAN expression and disrupted transport between cytoplasm and nucleus; a key event in Alzheimer's disease pathophysiology. *PLoS One*, **8**, e53349.
48. Godfrey, A.C., Xu, Z., Weinberg, C.R., Getts, R.C., Wade, P.A., DeRoo, L.A., Sandler, D.P. and Taylor, J.A. (2013) Serum microRNA expression as an early marker for breast cancer risk in prospectively collected samples from the Sister Study cohort. *Breast Cancer Res.*, **15**, R42.
49. Shi, W.L., Liu, Z.Z., Wang, H.D., Wu, D., Zhang, H., Xiao, H., Chu, Y., Hou, Q.F. and Liao, S.X. (2016) Integrated miRNA and mRNA expression profiling in fetal hippocampus with Downsyndrome. *J. Biomed. Sci.*, **23**, 48.
50. Kumar, S., Chawla, Y.K., Ghosh, S. and Chakraborti, A. (2014) Severity of hepatitis C virus (genotype-3) infection positively correlates with circulating microRNA-122 in patients sera. *Dis. Markers*, **2014**, 435476.
51. Livak, K.J. and Schmittgen, T.D. (2001) Analysis of relative gene expression data using real-time quantitative PCR and the $2^{-\Delta\Delta CT}$ method. *Methods*, **25**, 402–408.
52. Alhasan, A.H., Scott, A.W., Wu, J.J., Feng, G., Meeks, J.J., Thaxton, C.S. and Mirkin, C.A. (2016) Circulating microRNA signature for the diagnosis of very high-risk prostate cancer. *Proc. Natl. Acad. Sci. U.S.A.*, **113**, 10655–10660.